

Seismic Wave Propagation Simulation in a Poro-elastic Medium Using Spectral Method Elements in MPI-GPU Cluster: Study Case of Anticline Reservoir Trap

Sudarmaji¹, Indra Rudianto², Muhammad Kautsar Rahmareza³ and Yosua Alfontius⁴

Department of Physics, Faculty of Mathematics and Natural Sciences, Gadjah Mada University, Yogyakarta, Indonesia

¹ajisaroji@ugm.ac.id, ²indrarudianto.official@gmail.com, ³kautsar.rezha@gmail.com, ⁴alfontiusyosua@gmail.com

ABSTRACT

Modeling 2D seismic wave propagation using spectral element method on MPI-GPU clusters has been implemented and can complete the problem of the elastic poro-elastic medium model. Free surface boundary conditions and the absorption layer will use the CPML method. Seismic wave propagation simulation in the hybrid elastic poro-elastic medium has been carried out on hydrocarbon reservoir models with anticline type. In reservoir rocks that have a poro-elastic medium, there will be a fast and slow P wave. While in non-reservoir rocks that have elastic medium, only P fast waves are observed. The computation time for an anticline type reservoir model with dimensions of 1 km x 1.5 km using MPI 4 nodes cluster with 48 CPU cores is 3 minutes 48 second.

INTRODUCTION

In recent years, numerical simulation of wave propagation in fluid-saturated poroelastic media has received more attention as its importance in geophysical exploration and reservoir characterization. Biot's theory [1,2] is the basis for the numerical simulation of wave propagation in fluid saturated poroelastic media. The finite-difference (FD) method for Biot's equations has been formulated in several ways, central difference FD method in displacement [3], velocity-stress predictor corrector FD method [4]. An unsplit convolutional perfectly matched layer (CPML) is the stable new an absorbing boundary condition [5]. Numerical modeling of 2D seismic wave propagation in fluid-saturated porous media based on finite difference method using Graphics Processing Unit (GPU) has been implemented to simple hydrocarbon reservoir model [6].

Due to the irregular shape of reservoir distribution, implementation finite difference method has some limitation. Another numerical method which could address the irregular shape of reservoir distribution is a finite element and spectral element method. These methods have been successfully applied in many areas of seismic modeling [7-10]. Spectral element method also has been implemented to accommodate a considerable irregular shape of surface topography [11-12]. To accommodate the irregular shape of reservoir distribution, we use the spectral-element method (SEM) to simulate seismic wave propagation in the hydrocarbon reservoir model especially anticline reservoir model type. It uses a weak formulation for solving elastic wave equation and naturally incorporates the irregular shape of reservoir conditions.

THEORY

Strong Formulation

Wave propagation in the poroelastic medium is defined by the following Biot equation:

$$\bar{\rho} \partial_t^2 \bar{\mathbf{u}}_s + \rho_f \partial_t^2 \bar{\mathbf{w}} = \nabla \cdot \bar{\mathbf{T}} + \mathbf{f}, \quad (1)$$

$$m \partial_t^2 \bar{\mathbf{w}} + \rho_f \partial_t^2 \bar{\mathbf{u}}_s + \eta_f \mathbf{k}^{-1} \cdot \partial_t \bar{\mathbf{w}} = \nabla \cdot \bar{\mathbf{T}}_f + \mathbf{f}, \quad (2)$$

with $\bar{\rho}$ is the average density defined by the equation

$$\bar{\rho} = (1 - \phi)\rho_s + \phi\rho_f \quad (3)$$

with ϕ is porosity, ρ_s is density of solid rock, and ρ_f is the density of fluid. Solid rock displacement is symbolized by $\bar{\mathbf{u}}_s$, $\bar{\mathbf{w}}$ is the displacement of the fluid relative to the displacement of solid rock weighted by porosity,

$$\bar{\mathbf{w}} = \phi(\bar{\mathbf{u}}_f - \bar{\mathbf{u}}_s). \quad (4)$$

Average macroscopic stress $\bar{\mathbf{T}}$ defined by equation

$$\bar{\mathbf{T}} = (1 - \phi)\bar{\mathbf{T}}_s + \phi\bar{\mathbf{T}}_f. \quad (5)$$

The m symbol in equation 2 is defined by $m = \rho_f c / \phi$, with c is tortuosity, η_f is fluid viscosity fluida, k is permeability, $\bar{\mathbf{T}}_f$ is fluid stress, dan \mathbf{f} is wave source. In isotropic media,

$$\bar{\mathbf{T}} = \mathbf{G} : \nabla \bar{\mathbf{u}}_s + C \nabla \cdot \bar{\mathbf{w}} \mathbf{I}, \quad (6)$$

and

$$\bar{\mathbf{T}}_f = -\bar{\rho}_f \mathbf{I} = (C \nabla \cdot \bar{\mathbf{u}}_s + M \nabla \cdot \bar{\mathbf{w}}) \mathbf{I}, \quad (7)$$

with

$$C = \frac{\kappa_s(\kappa_s - \kappa_{fr})}{D - \kappa_{fr}}, \quad (8)$$

$$M = \frac{\kappa_s^2}{D - \kappa_{fr}}, \quad (9)$$

$$D = \kappa_s \left[1 + \phi \left(\frac{\kappa_s}{\kappa_f} - 1 \right) \right], \quad (10)$$

with κ_s is the bulk modulus of solid rock, κ_f is the bulk modulus of fluid, and κ_{fr} is the bulk modulus of frame. Tensor \mathbf{G} defined by

$$G_{ijkl} = (H - 2\mu_{fr})\delta_{ij}\delta_{kl} + \mu_{fr}(\delta_{ik}\delta_{jl} + \delta_{il}\delta_{jk}), \quad (21)$$

with

$$H = \frac{(\kappa_s - \kappa_{fr})^2}{D - \kappa_{fr}} + \kappa_{fr} + \frac{4}{3}\mu_{fr}, \quad (32)$$

with μ_{fr} is a shear modulus of the frame.

Wave source \mathbf{f} could be written as tensor momen like :

$$\mathbf{f} = -\mathbf{M} \cdot \nabla \delta(\mathbf{x} - \mathbf{x}_s) S(t). \quad (13)$$

The location of the source point is denoted by \mathbf{x}_s , the distribution of the Dirac delta located in \mathbf{x}_s is denoted by $\delta(\mathbf{x} - \mathbf{x}_s)$, and the time function of the source is denoted by $S(t)$.

Weak Formulation

In weak formulations, the equations of motion and implementation of boundary conditions are solved in an integral form. Weak formulations are obtained by multiplying dot equations 1 and 2 with any vector test $\tilde{\mathbf{u}}$ and $\tilde{\mathbf{w}}$ respectively, integrating partially on the volume model Ω , and implementing the wave source in equation 4. This gives

$$\begin{aligned} \int_{\Omega} \tilde{\rho} \tilde{\mathbf{u}} \cdot \partial_t^2 \bar{\mathbf{u}}_s \, d^3 \mathbf{x} + \int_{\Omega} \rho_f \tilde{\mathbf{u}} \cdot \partial_t^2 \bar{\mathbf{w}} \, d^3 \mathbf{x} \\ = - \int_{\Omega} \nabla \tilde{\mathbf{u}} : \bar{\mathbf{T}} \, d^3 \mathbf{x} + \int_{\Gamma} \hat{\mathbf{n}} \cdot \bar{\mathbf{T}} \cdot \tilde{\mathbf{u}} \, d^2 \mathbf{x} + \mathbf{M} : \nabla \tilde{\mathbf{u}}(\mathbf{x}_s) S(t), \end{aligned} \quad (14)$$

$$\begin{aligned} \int_{\Omega} m \tilde{\mathbf{w}} \cdot \partial_t^2 \bar{\mathbf{w}} \, d^3 \mathbf{x} + \int_{\Omega} \rho_f \tilde{\mathbf{w}} \cdot \partial_t^2 \bar{\mathbf{u}}_s \, d^3 \mathbf{x} + \int_{\Omega} \eta_f \tilde{\mathbf{w}} \cdot (\mathbf{k}^{-1} \cdot \partial_t \bar{\mathbf{w}}) \, d^3 \mathbf{x} \\ = - \int_{\Omega} \nabla \tilde{\mathbf{w}} : \bar{\mathbf{T}}_f \, d^3 \mathbf{x} + \int_{\Gamma} \hat{\mathbf{n}} \cdot \bar{\mathbf{T}}_f \cdot \tilde{\mathbf{w}} \, d^2 \mathbf{x} + \mathbf{M} : \nabla \tilde{\mathbf{w}}(\mathbf{x}_s) S(t). \end{aligned} \quad (15)$$

with Γ covering free surface boundaries, boundaries between acoustic-poroelastic, elastic-poroelastic, and poroelastic-poroelastic media layers.

METHOD

2D Model and Mesh Implementation

The schematic model of anticline reservoir type and its mesh representation is shown in Figure 1. The dimension of the model is 1km x 1.5 km which contains some layers of rocks, such as: source rock (1), water reservoir (2), oil reservoir (3), gas reservoir (4), Seal Rock (5), Water Sand (6) and Shale (7). Zooming circle shows the interface between the elastic layer (seal rock) and poro-elastic layer (gas and oil reservoir). Each layer of rocks has their own physical properties. Table 1 shows physical properties of rock for the reservoir model. The mesh model has 12104 elements using interpolation for domains decomposition in the form of 4th order polynomials. Spectral element sizes range from 2m to 17m. Simulation is done by placing the source point at (600,-10) and deploying 3 receivers at x1(535,-10), x2(535,-450) and x3(535,-750).

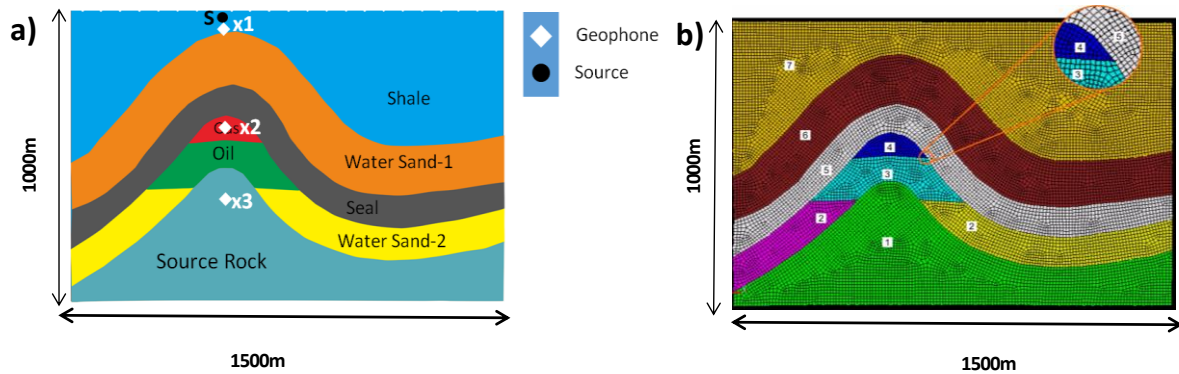


Figure 1. a. Schematic of the anticline reservoir model. b. Mesh Implementation model.

Tabel 1. Physical properties of rock for the reservoir model

Physical Properties	Elastik			
	Shale	Water sand 1	Seal	Source
Vp (m/s)	3000	3200	3400	3600
Vs (m/s)	1600	1850	1900	1950
ρs (kg/m3)	2750	2900	2950	2980
Poroelastik				
Physical Properties	gas	oil	water	
ρf (kg/m3)	150	650	1000	
μ	5.83 x 10 ⁹	6.2x10 ⁹	6.57x10 ⁹	
Kf	3.4x10 ⁷	7.41x10 ⁸	2.24x10 ⁹	
Ks	1.51 x 10 ¹⁰	1.51 x 10 ¹⁰	1.51 x 10 ¹⁰	
Kfr	9.96x 10 ⁹	9.86x 10 ⁹	1.28 x 10 ¹⁰	
a	1.2	1.2	1.2	
φ (%)	0.2	0.2	0.2	
η (Pa.S)	0.00001	0.03	0.003	

Simulation of the Anticline Reservoir Model

We use the SPEC2D software package [6] and decompose the model into 12104 hexahedral elements. In each spectral element we use the polynomial degree of $N = 4$, and thus each element contains $(N + 1)^3 = 125$ Gauss-Lobatto-Legendre (GLL) integration points. Total number of GLL points in the model is 14,124,456. The minimum and maximum distance between Gauss-Lobatto-Legendre integration points in the model is 2-17 m respectively. We use a Ricker wavelet as a source time function with dominant frequency is 20 Hz. The time step used is $\Delta t = 2.5 \times 10^{-5}$ ms, and we propagate the signal for 50000 time steps, thus total simulation time is 1.25 s.

The simulation is carried out on a GPU cluster with 4 NVIDIA QuadroK4000 graphics cards and 24 core processors Intel Xeon CPU E5-620 @2.4 GHz using MPI (Message Passing Interface) and CUDA (Compute Unified Device Architecture) at Computational and Seismic Laboratory, Geophysics Sub-Department, Gadjah Mada University.

RESULTS AND DISCUSSION

Seismic wave propagation simulation is done by placing the source at the source point (600m, 10m) and the receiver is 60 units arranged in the lateral array form at a depth of 10m from the surface to record reflection. The simulation uses a sampling time of 0.25×10^{-5} ms with an iteration of 50000 times. The source wave is a Ricker wavelet with a dominant frequency of 20Hz. The free surface boundary conditions and absorption layer use the CPML method. Figure 2 shows a snapshot of the vertical component velocity propagation of the anticline type reservoir model at time $t = 0.25$ s to $t = 0.5$ s.

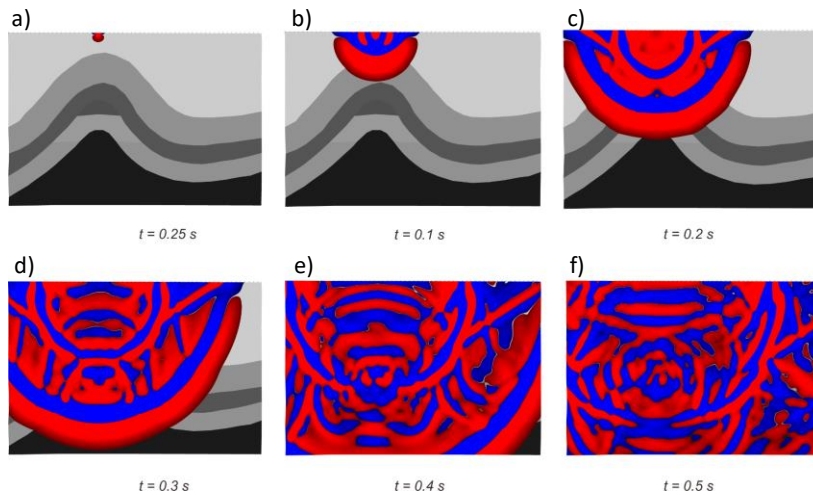


Figure 2. Snapshot of vertical component of velocity field propagation for the anticline reservoir model at time: a) $t=0.25$ s, b) $t=0.1$ s, c) $t=0.2$ s, d) $t=0.3$ s, e) $t=0.4$ s, f) $t=0.5$ s

Figure 3 shows velocity seismogram at receiver X1, receiver X2 and receiver X3. Symbol P_d^f is direct fast P-wave, P_{r1}^f is 1st reflection fast P-wave between shale and water sand-1, P_{r2}^f is 2nd reflection fast P-wave between water sand-1 and seal rock, P_{r3}^f is 3rd reflection fast P-wave between seal rock and gas reservoir, P_{r4}^f is 4th reflection fast P-wave between gas and oil reservoir, P_{r5}^f is 5th reflection fast P-wave oil reservoir and source rock, while P_d^s is direct slow P-wave. Direct slow P-wave P_d^s is only observed in receiver X2 which is located in poroelastic medium as gas reservoir. Due to receiver X1 and X3 are deployed at elastic medium, so direct slow P wave are not observed. In the Biot's poroelasticity, it's well known there are two compressional waves; i.e.: fast P wave and slow P wave. Fast P wave is compressional wave from solid frame, while slow P wave is compressional wave from fluid filling the rock pore.

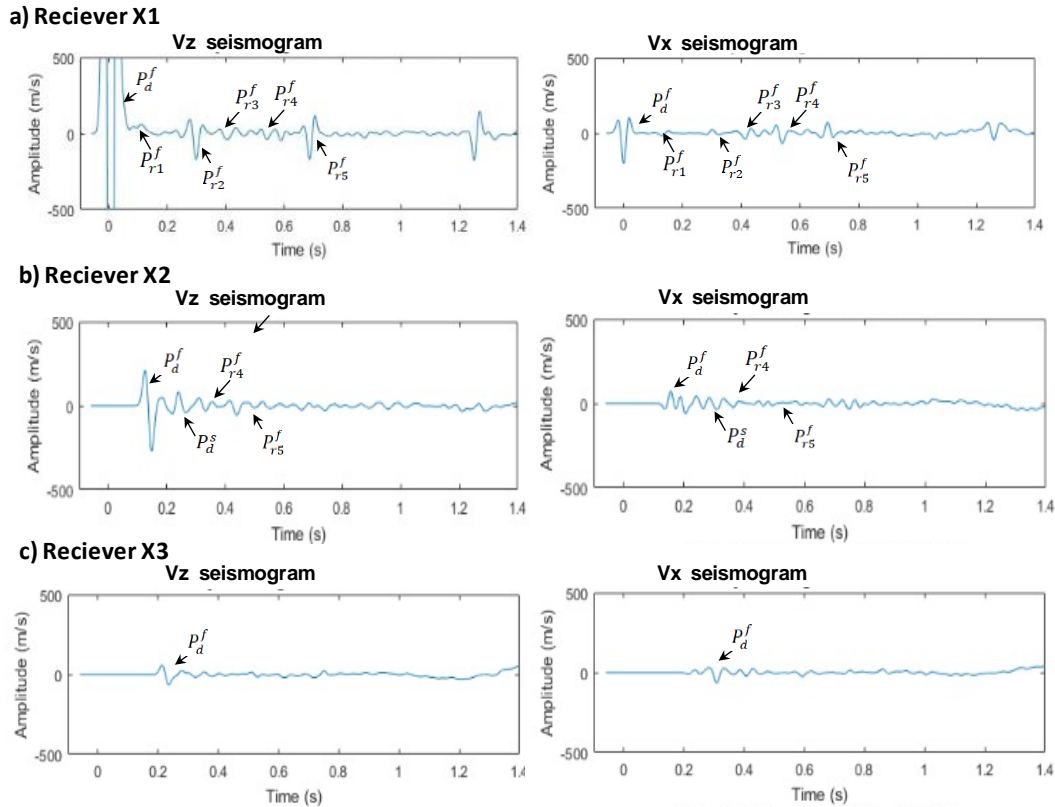


Figure 3. Velocity seismogram at: a) receiver X1, b) receiver X2 and c) receiver X3. Symbol P_d^f is direct fast P-wave, P_{r1}^f is 1st reflection fast P-wave, P_{r2}^f is 2nd reflection fast P-wave, P_{r3}^f is 3rd reflection fast P-wave, P_{r4}^f is 4th reflection fast P-wave, P_{r5}^f is 5th reflection fast P-wave and P_d^s is direct slow P-wave

CONCLUSIONS

We presented numerical modeling 2D seismic wave propagation using spectral element method on MPI-GPU clusters has been implemented and can complete the problem of elastic-poro elastic medium model. Seismic wave propagation simulation in the hybrid elastic-poroelastic medium has been carried out on the hydrocarbon reservoir model with anticline type. In reservoir rocks that have a poro elastic medium, there will be a fast and slow P wave. While in non-reservoir rocks that have elastic medium, only P fast waves is the observed.

In our future works, we intend to develop more realistic mesh implementation, enlarge and make more detail the dimension of the model, and include all currently available relevant hydrocarbon reservoir information in our model.

ACKNOWLEDGMENTS

We would like to express our gratitude to PT. Chevron Indonesia for hardware donations given to Geophysics Study Program, Gadjah Mada University.

REFERENCES

- 1 Biot, M.A., 1956a, Journal of the Acoustical Society of America, v. 28, 168-178.
- 2 Biot, M.A., 1956b, Journal of the Acoustical Society of America, v. 28, 179-191.
- 3 Zhu, X., and McMechan, G.A., 1991, Geophysics, Vol. 56, No.3, p. 328-339.

- 4 Dai, N., Vafidis, A. and Kanasevich, E.R., 1995, *Geophysics*, Vol.60, No.2 (March-April 1995), p.327-340.
- 5 Martin, R., Komatitsch, D., and Ezziani, A., 2008, *Geophysics*, vol. 73, no. 4, p. t51-t61
- 6 Sudarmaji, Sismanto, Waluyo and Soedijono B, 2016, *AIP Conf. Proc.* **1755** 100001-1-7
- 7 Komatitsch D and Tromp J 1999 *Geophys. J. Int.* **139** 806-22
- 8 Komatitsch D, Erlebacher G, Göddeke D and Michéa D 2010 *J. Comp. Phys.* **229** 7692-7714
- 9 Komatitsch D, Liu Q, Tromp J, Süß P, Stidham C and Shaw J H 2004 *Bull. Seismol. Soc. Am.* **94** 87206
- 10 Komatitsch D, Ritsema J and Tromp J 2002 *Science* **298** 1737-42
- 11 Sudarmaji, Rudianto, I., Nurcahya, B.E., 2018, *Journal of Physics: Conference Series* 1011(1), 012023
- 12 Sudarmaji, Rudianto, I., 2018, *Journal of Physics: Conference Series* 1011(1), 012034